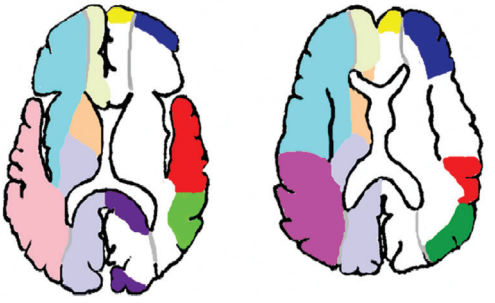

Vascular Territory	Brodmann's Area	Reading and Writing Deficits
Superior division MCA territory	Right BA 44/45	Viewer-centered neglect dyslexia
	Left BA 44/45	Impaired access to orthographic representations for written output and to phonological for spoken output; and impaired use of OPC/POC mechanisms (deep dyslexia and dysgraphia)
Inferior division MCA territory	Right BA 22	Stimulus-centered neglect dyslexia
	Left BA 22	Impaired access to semantic representations for reading and spelling
	Right BA 37	Stimulus-centered neglect dyslexia
	Left BA 37	Impaired access to modality-independent lexical processing, with impaired access to lexical representations for reading and spelling
	Right BA 39/40	Viewer-centered neglect dyslexia
	Left BA 39/40	Impaired access to OPC/POC mechanisms at word and subword levels (alexia with agraphia)
Posterior cerebral artery	Right splenium and striate cortex	unknown
	Left splenium and striate cortex	Alexia without agraphia; letter-by-letter reading

Plate 1 Neural regions associated with impairments of specific components of reading and spelling tasks, leading to different profiles of dyslexia and dysgraphia. The sites are shown in neuroradiographic convention, with the left hemisphere on the right side of the figure (OPC: orthography-to-phonology conversion; POC: phonology-to-orthography conversion).

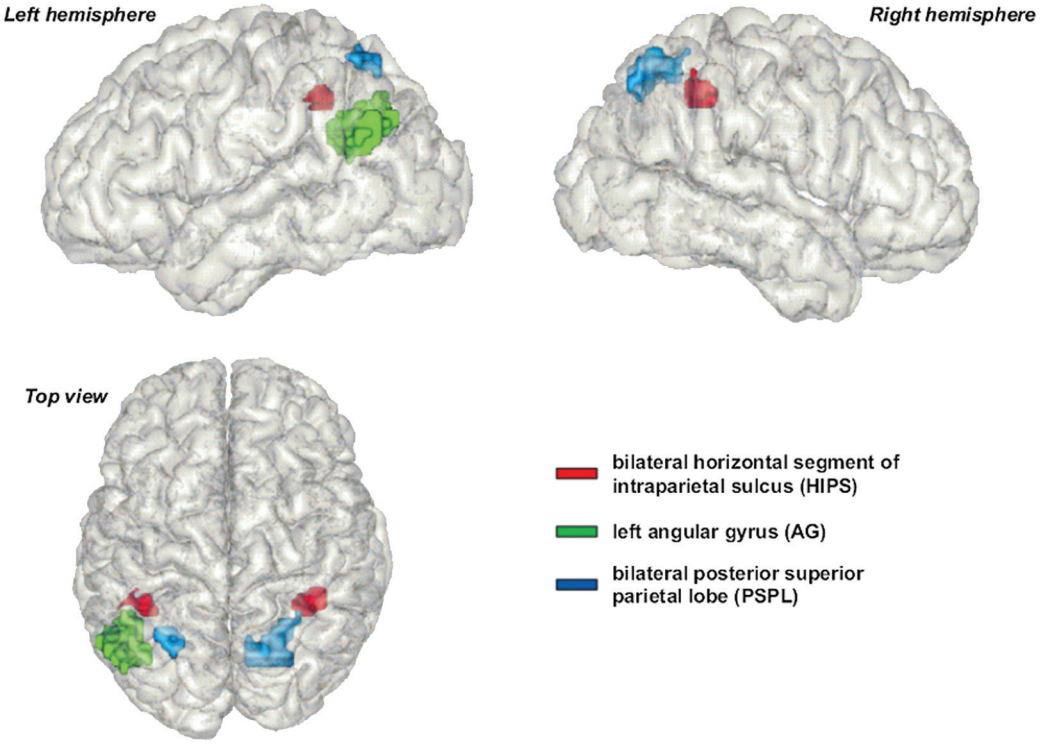

Plate 2 Three parietal circuits for number processing. Intersection of activations clusters from a metanalysis of fMRI activation studies. Red: the horizontal segment of the intraparietal sulcus (HIPS) was activated bilaterally in a variety of contrasts sharing a component of numerical quantity manipulation. Green: the left angular gyrus was activated during arithmetic tasks with a strong verbal component. Blue: the posterior superior parietal lobule was activated bilaterally in a few numerical tasks, overlapping with tasks of non-numerical visual attention shift. Reproduced from (Dehaene *et al*., 2003).

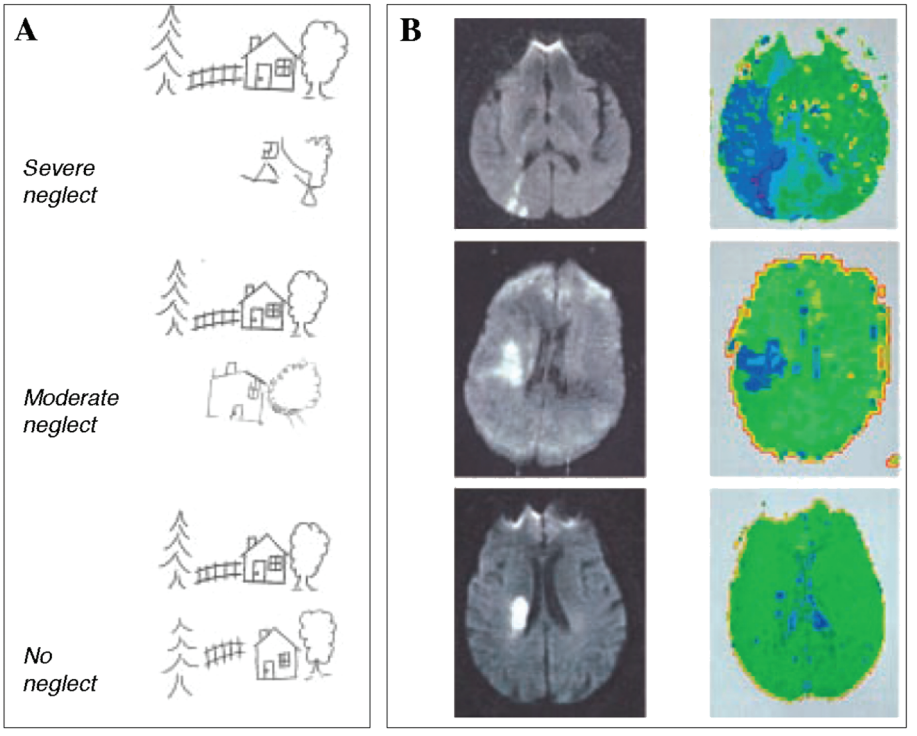

Plate 3 Differences in symptoms and lesions in three patients with acute right hemisphere stroke. (A) Copy of Ogden's multi-element scene from each patient, showing different degrees of severity in left spatial neglect, from severe (top) through to moderate neglect (middle) and no neglect (bottom). Performance in top row reveals both space-based/egocentric and object-based/allocentric omissions on the left side. (B) Abnormalities in diffusion weighted MRI (DWI, left column) and perfusion MRI (PWI, right column) in each patient, showing that stroke with similar volume of infracted tissue can be associated with different degrees of hypoperfusion in the right hemisphere (blue colored areas), corresponding with the different degrees of neglect severity.

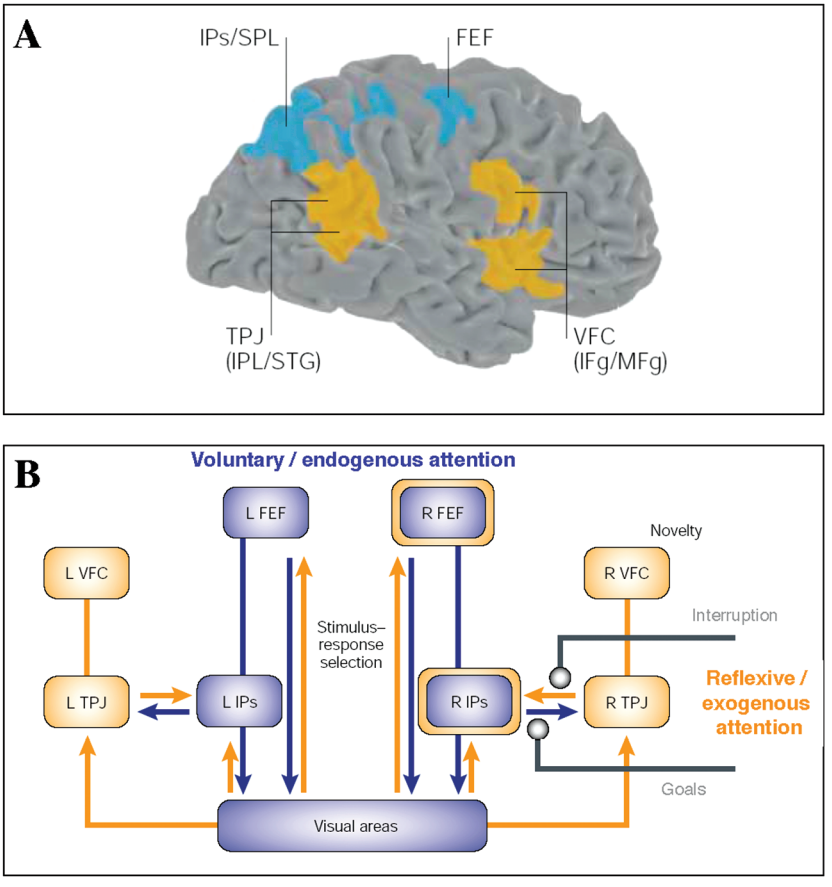

Plate 4 A recent neurocognitive model of visual spatial attention, proposed by Corbetta and Shulman (2002). (A) Two "superior" (blue) and "inferior" (yellow) networks of areas in parietal and prefrontal cortex have been identified by functional neuroimaging in normal subjects, and are also the most commonly damaged in neglect patients. (B) These two interconnected networks might be responsible for different attentional subcomponents, related to more intentional/endogenous (blue) and more reflexive/exogenous (yellow) aspects of spatial orienting. Abbreviations: FEF = frontal eye field (superior frontal gyrus), IFG = inferior frontal gyrus, MFG = middle frontal gyrus IPL = inferior parietal lobule, IPS = intraparietal sulcus, SPL = superior parietal lobule, TPJ = temporo-parietal junction, VFC = ventral pre-frontal cortex, L = left, R = right.

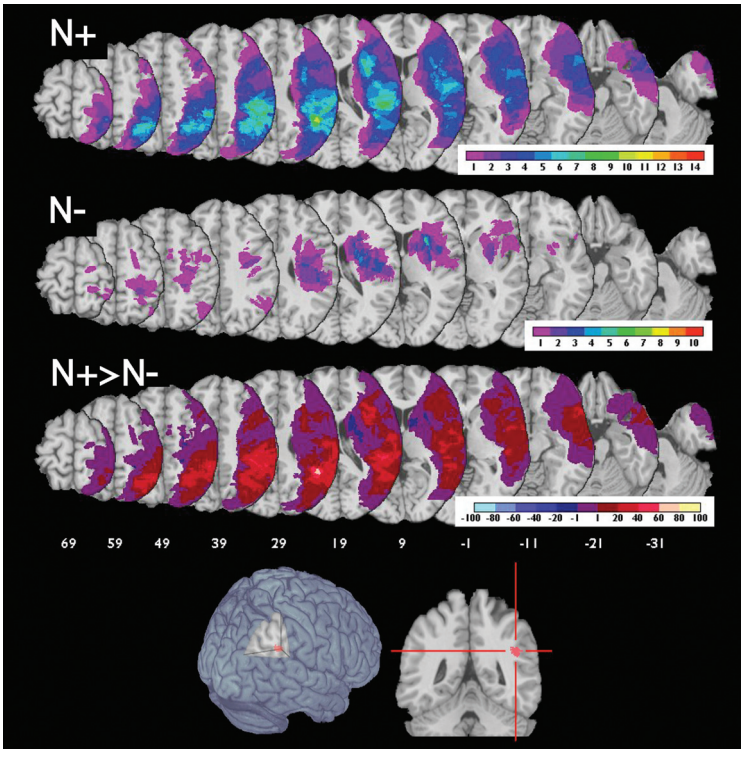

Plate 5 Overlap of lesions associated with neglect. Color bars indicate the number of patients with neglect (N+) and without neglect (N−) in the study of Mort *et al*. (2003).

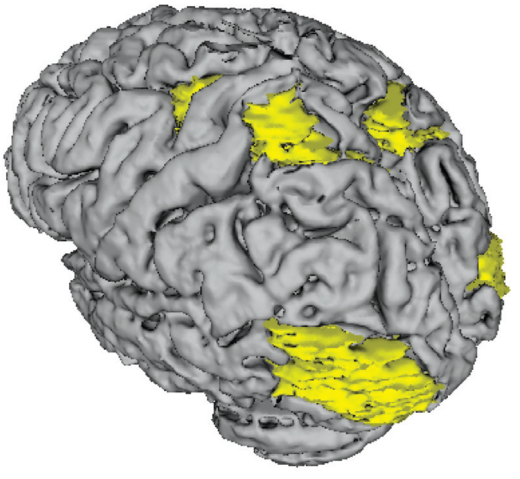

Plate 6 3D reconstruction of the lesions in the same patient. Lesions involve both the medial part of the posterior parietal cortex (upper lesion) and the lateral part of the occipital cortex (lower lesion).

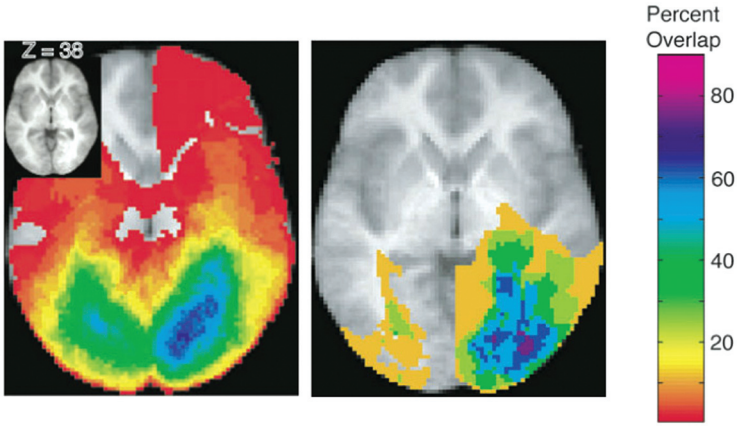

Plate 7 (Left)Lesion overlap of prosopagnosia cases. The prosopagnosia lesion overlap contains lesions from all cases with prosopagnosia regardless of achromatopsia diagnosis ($n = 52$). The inserts show the Talairach Z-coordinate at the average axial slice location. (Right) Lesion overlap of prosopagnosia cases with single disorder. The prosopagnosia lesion overlap (right) contains lesions from cases of prosopagnosia and intact color processing ($n = 8$). The scale bar indicates 1 cm. Figures taken from Bouvier, S.E. & Engel, S.A. (2005), with permission.